

# 확장형 칼만 필터를 이용한 인공위성 편대비행 상대 상태 추정

## Extended Kalman Filter Based Relative State Estimation for Satellites in Formation Flying

이 영 구\*, 방 효 충  
(Young-Gu Lee and Hyochong Bang)

**Abstract** : In this paper, an approach is developed for relative state estimation of satellite formation flying. To estimate relative states of two satellites, the Extended Kalman Filter Algorithm is adopted with the relative distance and speed between two satellites and attitude of satellite for measurements. Numerical simulations are conducted under two circumstances. The first one presents both chief and deputy satellites are orbiting a circular reference orbit around a perfectly spherical Earth model with no disturbing acceleration, in which the elementary relative orbital motion is taken into account. In reality, however, the Earth is not a perfect sphere, but rather an oblate spheroid, and both satellites are under the effect of  $J_2$  geopotential disturbance, which causes the relative distance between two satellites to be on the gradual increase. A near-Earth orbit decays as a result of atmospheric drag. In order to remove the modeling error, the second scenario incorporates the effect of the  $J_2$  geopotential force, and the atmospheric drag, and the eccentricity in satellite orbit are also considered.

**Keywords** : formation flying, relative state estimation,  $J_2$  geopotential disturbance, atmospheric drag, EKF

### I. Introduction

Spacecraft formation flying concepts have been studied since the beginning of space program in which the spacecraft rendezvous and docking maneuver onto each other were the main issues. The modern-day emphases of spacecraft formation flying have been put on the extended applications such as stereographic imaging, long baseline interferometry, and synthetic aperture radar(SAR) keeping a formation of several homogeneous/heterogeneous spacecraft. These formation flying have the advantages of structural flexibility in that even in case that one of the spacecraft which form the cluster fails, the mission can be carried out by reconfiguring the rest of the others, and the fine economical feasibility in that multiple satellites can provide for large size of aperture of radar dish without attempting to build up a large size radar dish by way of forming formation with its radius ranging from several meters to kilometers. In many missions, the global positioning system(GPS) is adopted so as to measure the relative position, but this system is applicable only to the near-Earth orbiting spacecraft. Some papers have made use of a vision-based navigation (VISNAV)system, which

provides line-of-sight(LOS) vectors between two satellites as a relative sensor measurement to surmount the drawback of GPS[15]. The objective of this paper is to provide a method for reliable autonomous satellites in formation flying without any assistance from external systems, just introducing additional simple devices(laser range finder and doppler radar) to the existing system. In this paper the relative distance combined with satellite's attitude, which provides line-of-sight(LOS) vector, and the speed between two satellites are adopted for relative sensor measurements. This measurement system is very attractive in that it is relatively simple and cheap providing enough accuracy for formation flying. To produce an accurate estimate of the true system state from the nonlinear measurement model, the Extended Kalman filter algorithm, which is probably the most widely used estimator for nonlinear systems, is adopted to provide the minimum mean squared error(MMSE) estimate. This paper consists of an overview of the relative orbit dynamics of two satellites with and without the effects of the  $J_2$  disturbing force, atmospheric drag and eccentricity of orbit, and the estimation of relative state variables using the Extended Kalman filter, and simulation results are followed.

\* 책임저자(Corresponding Author)

논문접수 : 2007. 8. 5., 채택확정 : 2007. 9. 1.

이영구, 방효충 : 한국과학기술원

(yglee@fdcl.kaist.ac.kr/hcbang@fdcl.kaist.ac.kr)

※ This work was supported by the Korea Science and Engineering Foundation(KOSEF) grant funded by the Korea government(MOST) (No. R01-2006-000-10189-0).

### II. Relative Orbit Dynamics

#### 1. The Hill-Clohessy-Wiltshire equations

The chief satellite is the one about which all other satellites are orbiting and can be virtual one, that is, there is no physical satellite occupying the chief position. The

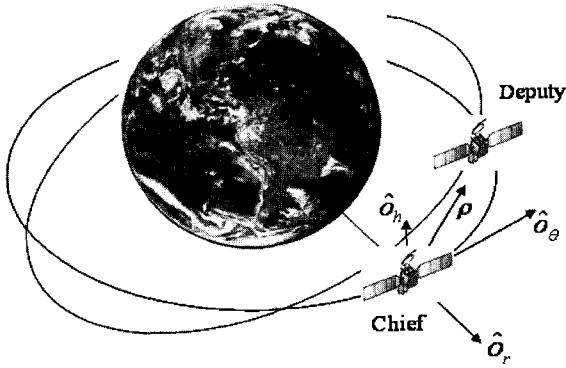


그림 1. Hill's 좌표계.

Fig. 1. Illustration of the Hill's frame.

remaining satellites, referred to as the deputy satellites, are orbiting the chief and constitute a formation with the chief as their center. The equations of relative motion start out with the following assumptions

1. The chief orbit is circular and the relative distance between the chief and deputy satellites is small compared with the chief orbit radius.
2. The Earth is perfectly sphere and homogeneous.
3. There is no force acting on the two bodies other than the inverse-squared gravitational force.

The relative motion of satellites are described in terms of cartesian coordinate vector in the chief satellite centered rotating reference frame, referred to as Hill frame with its vector components  $\{o_r, o_\theta, o_h\}$ , where  $o_r$  is in the orbit radius direction,  $o_\theta$  is in along track direction, and  $o_h$  completes the vector triad.

$$\rho = (x, y, z)^T \tag{1}$$

The deputy satellite position vector can be expressed as

$$r_d = r_c + \rho = (r_c + x)\hat{o}_r + y\hat{o}_\theta + z\hat{o}_h \tag{2}$$

where  $\hat{r}_c(t)$  and  $\hat{r}_d(t)$  are the inertial chief and deputy position vectors, respectively. The angular velocity vector of the rotating Hill frame relative to the inertial frame is given by  $\omega_{O/N} = \dot{f} \hat{o}_h$  with  $f$  being the chief frame true anomaly, where  $O$  means the Hill frame and  $N$  inertial frame. The acceleration vectors of the chief and deputy satellites, taking the second derivatives with respect to the inertial frame, are given

$$\ddot{r}_c = (\ddot{r}_c - r_c \dot{f}^2)\hat{o}_r = -\frac{\mu}{r_c^3} \hat{r}_c = -\frac{\mu}{r_c^2} \hat{o}_r \tag{3}$$

Further, the chief satellite acceleration vector can be expressed as

$$\ddot{r}_c = r_c \dot{f}^2 - \frac{\mu}{r_c^2} = r_c \dot{f}^2 \left(1 - \frac{\mu}{r_c^3 \dot{f}^2}\right) \tag{4}$$

$$= r_c \dot{f}^2 \left(1 - \frac{r_c \mu}{r_c^3 \dot{f}^2}\right) = r_c \dot{f}^2 \left(1 - \frac{r_c \mu}{H^2}\right) = r_c \dot{f}^2 \left(1 - \frac{r_c}{p}\right)$$

Because the chief orbit angular momentum magnitude can be expressed as  $h = r_c^2 \dot{f}$  and  $h$  is constant for unperturbed case (Keplerian motion), taking derivative of  $h$  with respect to time yields

$$\begin{aligned} \dot{h} &= 2r_c \dot{f} \dot{f} + r_c^2 \ddot{f} = 0 \\ \ddot{f} &= -2 \frac{\dot{f}}{r_c} \dot{f} \end{aligned} \tag{5}$$

Using equations (3), (4), and (5), the acceleration vector of the deputy satellite is reduced to

$$\begin{aligned} \ddot{r}_d &= [\ddot{x} - 2\dot{f}(\dot{y} - y\frac{\dot{f}}{r_c}) - x\dot{f}^2 - \frac{\mu}{r_c^2}] \hat{o}_r \\ &+ [\ddot{y} + 2\dot{f}(\dot{x} - x\frac{\dot{f}}{r_c}) - y\dot{f}^2] \hat{o}_\theta + \ddot{z} \hat{o}_h \end{aligned} \tag{6}$$

The deputy satellite motion can be expressed relative to the inertial frame as follows:

$$\ddot{r}_d = -\frac{\mu}{r_d^3} \hat{r}_d = -\frac{\mu}{r_d^3} \begin{pmatrix} r_c + x \\ y \\ z \end{pmatrix}_O \tag{7}$$

where  $r_d = \sqrt{(r_c + x)^2 + y^2 + z^2}$ .

The complete derivation of the relative equations of motion is provided in Ref. [1]. If the relative distance between the chief and the deputy satellites is small compared with the chief orbit radius, the relative orbit equations of motion are described as

$$\begin{aligned} \ddot{x} - x\dot{f}^2(1 + 2\frac{r_c}{p}) - 2\dot{f}(\dot{y} - y\frac{\dot{f}}{r_c}) &= 0 \\ \ddot{y} - y\dot{f}^2(1 - \frac{r_c}{p}) + 2\dot{f}(\dot{x} - x\frac{\dot{f}}{r_c}) &= 0 \\ \ddot{z} + \frac{r_c}{p} \dot{f}^2 z &= 0 \end{aligned} \tag{8}$$

where  $f$  is true anomaly of the chief satellite,  $p$  is semilatus rectum of the chief. If the chief orbit is chosen to be circular so that  $\dot{r}_c = 0$ ,  $p = r_c$  and  $e = 0$  then the well-known relative equations of motion, referred to as the Clohessy-Wiltshire (CW) equations are given by

$$\begin{aligned} \ddot{x} - 2n\dot{y} - 3n^2 x &= 0 \\ \ddot{y} - 2n\dot{x} &= 0 \\ \ddot{z} + n^2 z &= 0 \end{aligned} \tag{9}$$

where  $n$  is the mean orbital rate of the chief satellite, which is equal to the true anomaly rate for a circular reference orbit.

2. The modified HCW equations incorporating eccentricity in chief satellite

The modified HCW equations which incorporates the eccentricity of the chief satellite can be obtained from the general relative equations of motion described in section 2.1 and take the similar form of the original HCW equations by way of non-dimensionalizing them with respect to the chief orbit radius. The derivation is as follows[1]. The non-dimensional relative coordinates can be expressed as

$$u = \frac{x}{r_c}, v = \frac{y}{r_c}, w = \frac{z}{r_c} \tag{10}$$

The non-dimensional derivatives of  $u$ ,  $v$ , and  $w$  with respect to the chief orbit true anomaly are given by

$$\begin{aligned} \frac{\dot{x}}{r_c} &= u'f' + \frac{\dot{r}_c}{r_c} u & \frac{\ddot{x}}{r_c} &= u''f'^2 + u'f'^2 \left(1 - \frac{r_c}{p}\right) \\ \frac{\dot{y}}{r_c} &= v'f' + \frac{\dot{r}_c}{r_c} v & \frac{\ddot{y}}{r_c} &= v''f'^2 + v'f'^2 \left(1 - \frac{r_c}{p}\right) \\ \frac{\dot{z}}{r_c} &= w'f' + \frac{\dot{r}_c}{r_c} w & \frac{\ddot{z}}{r_c} &= w''f'^2 + w'f'^2 \left(1 - \frac{r_c}{p}\right) \end{aligned} \tag{11}$$

Applying the preceding equations to the general relative equations of motion yields

$$\begin{aligned} u''f'^2 + u'f'^2 \left(1 - \frac{r_c}{p}\right) - u'f'^2 \left(1 + 2\frac{r_c}{p}\right) - 2f'^2 \left(v'f' + v\frac{\dot{r}_c}{r_c} - v\frac{\dot{r}_c}{r_c}\right) &= 0 \\ f'^2 u'' - 2f'v' + u'f' \left(1 - \frac{r_c}{p} - 1 - 2\frac{r_c}{p}\right) &= 0 \\ u'' - 2v' + u \left(-\frac{3r_c}{p}\right) &= u'' - 2v' + u \left(-\frac{1 + e \cos f}{p}\right) = 0 \\ u'' - 2v' - \frac{3u}{1 + e \cos f} &= 0 \end{aligned} \tag{12}$$

After the same procedure for  $v$  and  $w$  components, we can finally obtain the following elegant non-dimensional form of relative equations as

$$\begin{aligned} u'' - 2v' - \frac{3u}{1 + e \cos f} &= 0 \\ v'' + 2u' &= 0 \\ w'' + w &= 0 \end{aligned} \tag{13}$$

These non-dimensional relative equations of motion take on a similar form of the HCW equations and take the eccentricity in the chief orbit into account.

### 3. The perturbing force modelling

#### 3.1 The modified HCW equations

The HCW equations derived in the previous section are based on the assumption that the Earth is perfectly sphere and its mass distribution is homogeneous. In reality, however, the Earth is not perfectly sphere, but rather an oblate spheroid due to its rotation, which causes variations in the gravitational field and the relative distance between

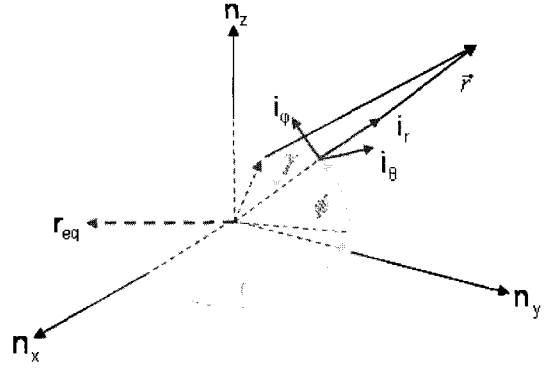


그림 2. 중력 포텐셜.

Fig. 2. Illustration of gravitational potential.

two satellites to be gradual increase. In this section the  $J_2$  disturbing force is applied to the right side of the Hill's equations as a forcing function. The gravitational potential of the earth, accounting for only latitude variation, takes on the following form

$$V = -\frac{Gm}{r} \left[ 1 - \sum_{k=2}^{\infty} \left(\frac{r_{eq}}{r}\right)^k J_k P_k(\sin \phi) \right] \tag{14}$$

where  $r_{eq}$  is the radius of the earth at its equator, the  $P_k$  are Legendre polynomial functions of order  $k$ , the  $J_k$  are constant coefficients, and  $\phi$  is the geocentric latitude. From Eq.(14) the disturbing potential is given by

$$\begin{aligned} V_{J_2} &= -\frac{\mu}{r} \left(\frac{r_{eq}}{r}\right)^2 J_2 P_2(\cos \phi) \\ &= -\frac{\mu}{r} \left(\frac{r_{eq}}{r}\right)^2 J_2 \left[\frac{1}{2}(3 \sin^2 \phi - 1)\right] \end{aligned} \tag{15}$$

From Fig. 2. it is evident that  $\sin \phi = \frac{z}{r}$ . Hence,

$$\begin{aligned} V_{J_2} &= \frac{\mu}{2r} \left(\frac{r_{eq}}{r}\right)^2 J_2 (1 - 3 \sin^2 i \sin^2 \theta) \\ &= \frac{\mu}{2r} \left(\frac{r_{eq}}{r}\right)^2 J_2 \left[1 - 3 \left(\frac{z}{r}\right)^2\right] \end{aligned} \tag{16}$$

The  $J_2$  induced gravitational acceleration acting on a satellite can be derived from the gravitational potential functions in the inertial reference frame in spherical coordinates

$$\begin{aligned} a_{J_2} &= \nabla V_{J_2} = \frac{\partial r_{eq}}{\partial r} \hat{r} + \frac{1}{r} \frac{\partial r_{eq}}{\partial \phi} \hat{i}_\phi + \frac{1}{r \cos \phi} \frac{\partial r_{eq}}{\partial \theta} \hat{i}_\theta \\ &= -\frac{3\mu r_{eq}^2}{2r^4} J_2 \begin{bmatrix} (1 - 3 \sin^2 \phi) \\ 2 \sin \phi \cos \phi \\ 0 \end{bmatrix} \end{aligned} \tag{17}$$

Using the direction cosine matrix transforming the inertial frame into the LVLH frame, the Eq. (17) can be expressed in the LVLH frame as follows

$$a_{\mathcal{L}} = -\frac{3\mu r^2}{2r^4} J_2 \begin{bmatrix} 1 - 3\sin^2 i \sin^2 \theta \\ 2\sin^2 i \sin \theta \cos \theta \\ 2\sin i \cos i \sin \theta \end{bmatrix} \quad (18)$$

Substituting Eq. (18) into Eq. (9) brings forth the following equations

$$\begin{aligned} \ddot{x} - 2n\dot{y} - 3n^2x &= -k(1 - 3\sin^2 i \sin^2 \theta) \\ \ddot{y} - 2n\dot{x} &= -2k\sin^2 i \sin \theta \cos \theta \\ \ddot{z} + n^2z &= -2k\sin i \cos i \sin \theta \end{aligned} \quad (19)$$

where  $k = \frac{3\mu r^2}{2r^4} J_2$  and  $n = \sqrt{\frac{\mu}{r^3}}$

The  $\mathcal{L}$  term in the right side of Eq. (19) is based on the assumption that the deputy satellite is in the vicinity of the chief satellite such that two satellites experience the same disturbing force. For reducing the modeling error, the gradient term  $\nabla J_2(r_c)$  must be taken into account. The addition of the  $\nabla J_2(r_c)$  term, however, causes the differential equations of motion not to be solved analytically because it has time varying coefficients. In Ref. [2], the  $\nabla J_2(r_c)$  term is time averaged over a single period to resolve this problem. while the analytical solution of the differential equations of motion can be obtained, this causes another problem of mismatching of the orbital periods of the two satellites. In Ref. [2], the author also suggests a solution to this problem via “speeding up” the reference satellite by amount of time averaged components of the  $\mathcal{L}$ .

$$\ddot{r}_c = g(r_c) + \frac{1}{2\pi} \int_0^{2\pi} J_2(r_c) d\theta \quad (20)$$

Applying this equation to relative motion brings forth a linear, constant coefficient, coupled differential equation that can be solved analytically. And the final differential equations of motion take on the form that

$$\begin{bmatrix} \ddot{x} - 2(nc)\dot{y} - (5c^2 - 2)n^2x \\ \ddot{y} + 2(nc)\dot{x} \\ \ddot{z} + (3c^2 - 2)n^2z \end{bmatrix} = J_2(r_c) - \frac{1}{2\pi} \int_0^{2\pi} J_2(r_c) d\theta \quad (21)$$

Further details on the preceding are provided in Ref. [2].

### 3.2 The modified HCW equations accommodating atmospheric Drag

In this section, we take the effects of atmospheric drag on the satellites formation into account. The previous works done by Carter-Humi will be reviewed and applied to system dynamics for estimating the relative states between two satellite in the following section. In an inertial frame the equations of motion of the satellite in orbit can be expressed as

$$\ddot{r}_c = -f(r_c)r_c - \alpha g(r_c) \dot{r}_c \quad (22)$$

The first term on the right accounts for gravitational

acceleration due to a central force field and the second indicates atmospheric drag acceleration. The scalar  $\alpha$  is a constant associated with the atmospheric drag coefficient and the geometry of the satellite. The function  $g$  stands for atmospheric density, and assumed to be dependent only on altitude. The preceding equation can be rewritten as

$$\ddot{r}_c = -f(r_c)r_c - \alpha g(r_c) \dot{r}_c \quad (23)$$

under the assumption that the orbit is initially not of high eccentricity but decay due to drag, in which the magnitude of the radial velocity is very small compared with that of the transverse velocity, that is,  $|\dot{r}_d| \ll r_c \dot{\theta}$ . In the same way the motion of a deputy satellite is governed by

$$\ddot{r}_d = -f(r_d)r_d - \beta g(r_d) \dot{r}_d \quad (24)$$

where  $r_d = r_c + r$  and  $r$  is the relative position vector between the chief and the deputy satellites, and  $\beta$  is the atmospheric drag constant associated with the deputy. The transformation to a rotating frame and changing independent variables from time  $t$  to the chief satellite's true anomaly with some algebraic processes lead to the simpler form

$$\begin{aligned} x'' &= 2y' - [f'(r_c)r_c / \omega^2 + \alpha g(r_c)r_c' + \beta g'(r_c)r_cr_c'] \\ &\quad - (\beta - \alpha)g(r_c)[(r_cx)' + r_c'x - r_cy + r_cy' / E(\theta)] \\ y'' &= -2x' - r_c[\alpha g(r_c) + \beta g'(r_c)r_c]y \\ &\quad - (\beta - \alpha)g(r_c)[2r_cy + (r_cy)' + r_c^2E(\theta)] \\ z'' &= -z - (r_cz)'(\beta - \alpha)g(r_c) \end{aligned} \quad (25)$$

where  $E(\theta)$  is a transformation for simplifying the governing equations, and further details are given in Ref.[9]. In a Newtonian gravitational field,  $f(r_c) = \mu/r_c^3$  and  $g(r_c) = 1/r_c$ . The acceleration due to the atmospheric drag is, therefore,  $-(\alpha/r_c)\dot{r}_c$ . Under the assumption that the chief and the deputy satellites are close enough to each other, they have identical drag constants, that is  $\alpha = \beta$ , so that we have the following elegant form

$$\begin{aligned} x'' &= 2y' + \frac{3(1+4\alpha^2)x}{1 + \epsilon e^{-2\omega\theta} \cos(\theta - \theta_0)} \\ y'' &= -2x' \\ z'' &= -z \end{aligned} \quad (26)$$

where  $\epsilon$  is eccentricity of orbit.

### III. Relative State Estimation

In this section, the estimation of relative state between two satellites will be presented using EKF as estimators. From given system dynamic and measurement models, we would like to obtain the minimum mean squared error(MMSE) estimate of the system state vector. The EKF

makes use of linearized system dynamic and measurement models, assuming that the non-linearities in system and measurement models are sufficiently smooth. To obtain the MMSE, The EKF is applied to the nonlinear discrete time system of the form

$$\begin{aligned} x(k+1) &= f[x(k), v(k), k], \\ z(k) &= h[x(k), k] + w(k) \end{aligned} \quad (27)$$

where  $x(k)$  is the state of the system at time step  $k$ ,  $v(k)$  is the system noise,  $z(k)$  is the measurement vector, and  $w(k)$  is the measurement noise. The control input are not considered here. It is assumed that all the noises are zero-mean gaussian and there is no correlation between them.

$$\begin{aligned} E[v(i)v^T(j)] &= \delta_{ij}Q(i), \\ E[w(i)w^T(j)] &= \delta_{ij}R(i), \\ E[v(i)w^T(j)] &= 0, \text{ for all } i, j \end{aligned} \quad (28)$$

where  $Q$  and  $R$  represent the covariances of system noise ( $w(k)$ ), measurement noise( $v(k)$ ), respectively.

The problem of determining the MMSE is equivalent to calculate the conditional mean from given measurements. The EKF propagates the first two moments of the distribution of  $x(k)$ , mean and covariance, through the system and measurement equations, recursively, and then the transformed mean and covariances are updated with new current measurement. The mean is transformed through non-linear system and the covariance is transformed through linearized equations. The preceding can be summarized as follows [13,14]

1. Prediction quantities at time step  $k$

$$\begin{aligned} \hat{x}(k+1|k) &= f[\hat{x}(k|k), k+1] \\ P(k+1|k) &= J_f P(k|k) J_f^T + Q(k+1) \\ \hat{z}(k+1|k) &= H \hat{x}(k+1|k), k+1 \\ P_w(k+1|k) &= J_h P(k+1|k) J_h^T + R(k+1) \end{aligned} \quad (29)$$

where  $J_f, J_h, P_{\nu\nu}$  denote the Jacobian matrices of the process and measurement models, and the predicted measurement covariance, respectively.

2. Estimated quantities at time step  $k+1$  with the new current measurement at time step  $k+1$

$$\begin{aligned} \hat{x}(k+1|k+1) &= \hat{x}(k+1|k) + W(k+1)\nu(k+1) \\ P(k+1|k+1) &= P(k+1|k) - W(k+1)P_{\nu\nu}(k+1|k)W(k+1) \\ \nu(k+1) &= z(k+1) - \hat{z}(k+1|k) \\ W(k+1) &= P_{\nu\nu}(k+1|k)P_w^{-1}(k+1|k) \end{aligned} \quad (30)$$

where  $W(k+1)$ ,  $\nu(k+1)$ , and  $P_{\nu\nu}$  represent the Kalman gain, the difference between actual measurement and the predicted measurement, and the cross-covariance, respectively.

In this paper the relative distance, speed, and the attitude

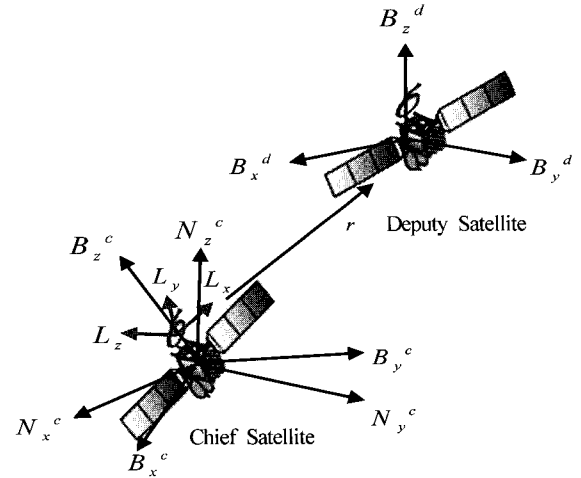


그림 3. 두 위성간 상대 위치 측정 도식.

Fig. 3. Illustration of measurement geometry between two satellites.

of the chief satellite are to be used for measurements to estimate the relative state, which enable an autonomous formation flying without any assistance from external system such as GPS, just employing the laser range finder, doppler radar, and the attitude information from its own system. This measurement system is very attractable in that it is relatively simple and cheap providing enough accuracy for formation flying. Fig. 3. shows the illustration of measurement geometry between two satellites.

$N^c, B^c, B^d$  and  $L$  denote LVLH frame, chief satellite's body frame, deputy satellite's body frame and sensor frame, respectively. We assume that the origins of  $N^c, B^c, L$  frames coincide with each other because the offset distance of laser range finder from the center of the chief satellite is small enough compared to the relative distance between two satellites. The relative position vector between two satellite can be obtained through the coordinate transformation, which makes use of the information of relative distance and the attitude of chief satellite equipped with laser range finder.

$$R^{LVLH} = C_{B_c}^{LVLH} C_L^{B_c} \begin{bmatrix} r \\ 0 \\ 0 \end{bmatrix}^L \quad (31)$$

where  $C_{B_c}^{LVLH}, C_L^{B_c}$  represent the rotational matrices which convert a vector expressed in the chief satellite's body frame to a vector expressed in the LVLH frame and convert a vector expressed in the sensor frame to a vector expressed in the chief satellite's body frame, respectively, and  $R^{LVLH}, r$  denote the relative position vector between two satellites expressed in the LVLH frame and relative distance measured from laser range finder, respectively.

We assume that the laser range finder is aligned along the x axis of sensor frame and the attitude of chief satellite with respect to the LVLH frame is known very accurately to the extent of 0.001s degree from secondary attitude measuring devices such as star sensor and sun sensor. The relative vector obtained in Eq. (31) suffices to estimate the relative state, however, for the sake of information redundancy we adopt relative speed as additional measurement, which is obtained from a doppler radar. The measurement vector is given by

$$h = [R^{LVLH^T} \dot{\rho}]^T \quad (32)$$

where  $\dot{\rho} = (\dot{x}\hat{x} + \dot{y}\hat{y} + \dot{z}\hat{z})/\rho$  represents the relative range rate.

Note that the measurement vector is originally linear, but becomes nonlinear one due to the augmented additional measurement. Taking the partial derivative of the measurement vector with respect to the states yields the output sensitivity equations as

$$\frac{\partial h}{\partial x_{i=\hat{x}_k}} = \begin{bmatrix} 1 & 0 & 0 & 0 & 0 & 0 \\ 0 & 1 & 0 & 0 & 0 & 0 \\ 0 & 0 & 1 & 0 & 0 & 0 \\ -\frac{x\dot{\rho}}{\rho^2} + \frac{\dot{x}}{\rho} & -\frac{y\dot{\rho}}{\rho^2} + \frac{\dot{y}}{\rho} & -\frac{z\dot{\rho}}{\rho^2} + \frac{\dot{z}}{\rho} & \frac{x}{\rho} & \frac{y}{\rho} & \frac{z}{\rho} \end{bmatrix} \quad (33)$$

where  $\rho = \sqrt{x^2 + y^2 + z^2}$  denotes relative range between two satellites.

**IV. Simulation Results**

In this section the simulation results are presented, which

표 1. 시뮬레이션 파라미터.

Table 1. Simulation parameters.

		Simulation Data		
Chief Satellite	eccentricity	0.001/0.03		
	Altitude	700km		
	Inclination	20deg		
EKF	Q	$diag[(10^{-4}/r_c)^2]_{6 \times 6}$ $r_c$ is the radius of the chief		
	R	I	$diag[(3 \times 10^{-5}/r_c)^2]_{3 \times 3}$ $r_c$ is the radius of the chief	
		II	$diag[(3 \times 10^{-4}/r_c)^2]_{3 \times 3}$ $r_c$ is the radius of the chief	
	Initial State Error	I	$[5 \times 10^{-3} \ 3 \times 10^{-3} \ 4 \times 10^{-3} \ 1 \times 10^{-6} \ 1 \times 10^{-6} \ 1 \times 10^{-6}]^T$	
		II	$[5 \times 10^{-3} \ 3 \times 10^{-3} \ 4 \times 10^{-3} \ 1 \times 10^{-3} \ 1 \times 10^{-3} \ 1 \times 10^{-3}]^T$	
P(0)		$[x(0) - \hat{x}(0)][x(0) - \hat{x}(0)]^T$		

show the performance of EKF as estimator to estimate the relative state with the relative range coupled with the attitude of satellite, and the speed between two satellites, considering the effects of the  $\mathcal{J}$  geopotential disturbing force, atmospheric drag and eccentricity in the chief satellite's orbit. The initial conditions and methodologies described in section 2 are chosen to guarantee that the relative orbit geometry remains bounded. The simulation is conducted for 2 orbit periods with a interval of 1 degree. The measurements have been used to update the a priori states with the same rate of system propagation. The simulation parameters are described in Table 1.

Fig. 4-9. show the true and the estimated relative motions between the chief and deputy satellites under the effect of  $\mathcal{J}$  geopotential disturbance and atmospheric drag with eccentricity of 0.001/0.03, respectively. It turns out that the application of the EKF to the relative state estimation with range coupled with satellite's attitude and

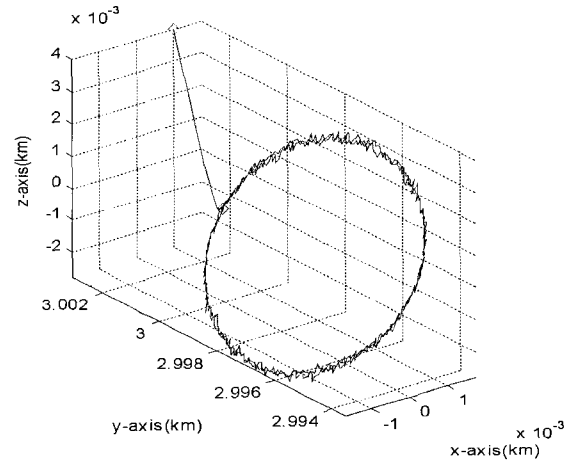


그림 4. 추정 상대 위치(이심률 : 0.001).

Fig. 4. Estimated position with eccentricity of 0.001.

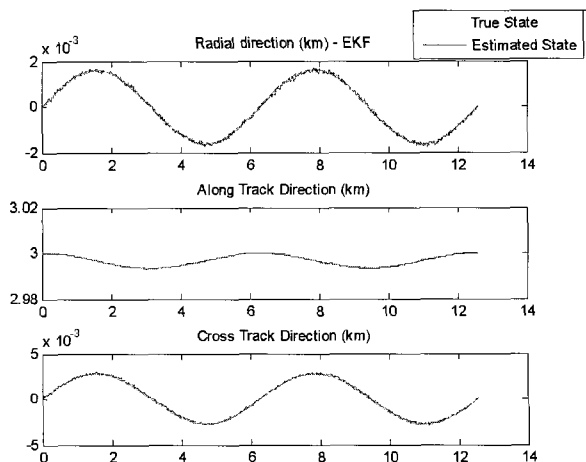


그림 5. 실제 및 추정 상대 위치 비교(이심률 : 0.001).

Fig. 5. True and estimated position with eccentricity of 0.001.

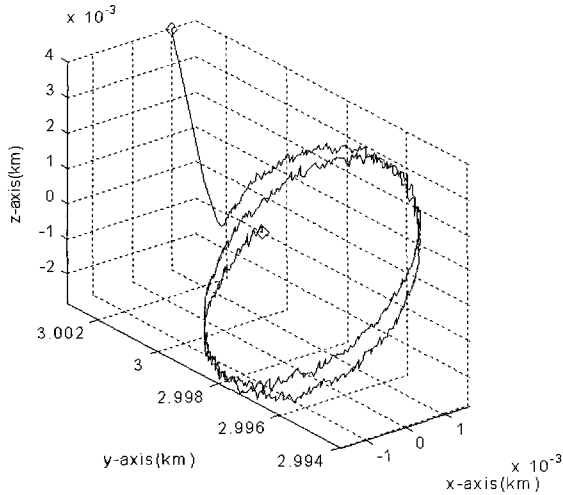


그림 6. 추정 상대 위치(이심률 : 0.03).

Fig. 6. Estimated position with eccentricity of 0.03.

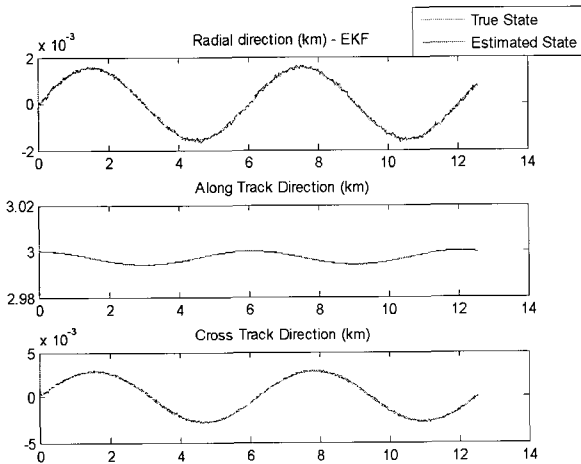


그림 7. 실제 및 추정 상대 위치 비교(이심률 : 0.03).

Fig. 7. True and estimated position with eccentricity of 0.03.

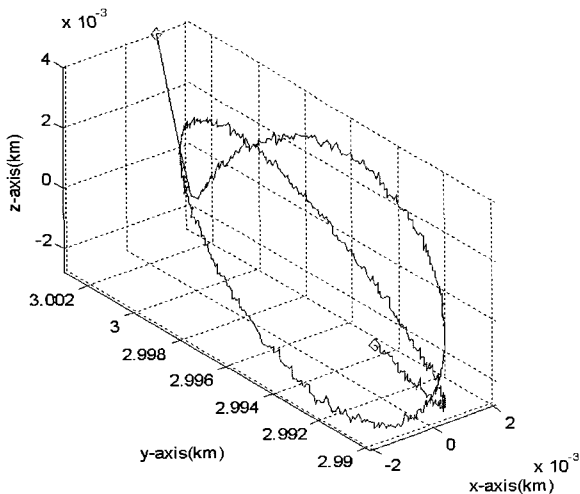


그림 8. 대기 항력 및  $J_2$  효과를 고려한 추정 상대 위치.

Fig. 8. Estimated position with atmospheric drag and  $J_2$  effect.

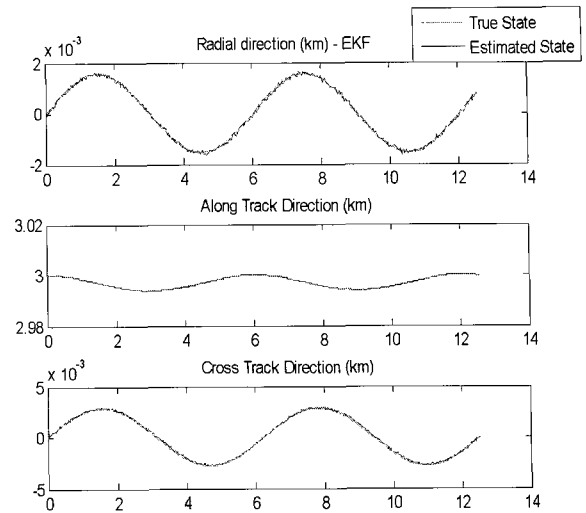


그림 9. 대기 항력 및  $J_2$  효과를 고려한 실제 및 추정 상대 위치 비교.

Fig. 9. True and estimated position with atmospheric drag and  $J_2$  effect.

speed information as their measurements brings forth good performances for moderate errors in the initial states and the measurements.

### V. Conclusion

In this paper Extended Kalman Filter has been designed to estimate the relative states of two satellites taking account of the effect of  $J_2$  geopotential disturbing force, atmospheric drag, and the eccentricity in the chief orbit, exploiting the relative range, speed, and the attitude of chief satellite as measurements.

Simulation results indicate that it is possible to estimate all the state variables through the EKF using aforementioned measurements with moderate errors without any additional information from external sources.

### References

- [1] H. Schaub and J. L. Junkins, "Analytical Mechanics of Space Systems," *AIAA, Educational Series*, 2003.
- [2] S. Schweighart and R. Sedwick, "A perturbative analysis of geopotential disturbances for satellite cluster formation flying," *IEEE Aerospace Conference*, vol. 21, pp. 1001-1019, 2001.
- [3] S. Schweighart and R. Sedwick, "High-fidelity linearized  $J_2$  model for satellite formation flight," *Journal of Guidance, Control and Dynamics*, vol. 25, no. 6, 2002.
- [4] John E. Prussing and Bruce A. Conway, *Orbital Mechanics*, Oxford University Press, New York, 1993.
- [5] J. Tschauner and P. Hempel, "Rendezvous zu ein min elliptischer bahn umlaufenden ziel," *Astronautica*, vol. 11, no. 2, 1965.

- [6] Richard H. Battin, "An Introduction to the Mathematics and Methods of Astrodynamics," AIAA Education Series, 1999.
- [7] Vladimir A. Chobotov, "Orbital mechanics 2nd edition, AIAA education series," 1996.
- [8] D. A. Vallado, *Fundamentals of Astrodynamics and Applications*, McGraw-Hill, New York, 1997.
- [9] Thomas Carter, "Clohessy-wiltshire equations modified to include quadratic drag," *Journal of Guidance, Control and Dynamics* vol. 25, no. 6, 2002.
- [10] M. Humi and T. Carter, "Models of motion in a central force field with quadratic drag," *Journal of Celestial Mechanics and Dynamical Astronomy*, vol. 84, no. 3, 2002.
- [11] A. Gelb(ed), *Applied Optimal Estimation*, MIT Press, Cmbridge, MA, 1974.
- [12] Mohinder S. Grewal and Angus P. Andrews, *Kalman Filtering : Theory and Practice(2nd Ed.)*, Wiley, New York, 2001.
- [13] S. J. Julier and J. K. Uhlmann, "A new extension of the Kalman filter to nonlinear systems," *American Control Conference*, pp. 1628-1632, 1995.
- [14] S. J. Julier and J. K. Uhlmann, "A general method for approximating nonlinear trnasformations of probability distributions," Available: <http://www.robots.ox.ac.uk/~siju>
- [15] S.-G. Kim, "Kalman filtering for relative spacecraft attitude and position estimation," *Journal of Guidance, Control and Dynamics*, vol. 30, no. 1, 2007.

### 이 영 구



2002년 해군사관학교 전산학과 졸업. 2006년~현재 한국과학기술원 항공우주 공학석사과정. 관심분야는 인공위성 편대비행 궤도 추정 및 제어.



### 방 효 충

1985년 서울대학교 졸업. 1987년 동 대학 대학원 석사. 1992년 Texas A&M University 항공우주공학 박사. 1992년 7월~1994년 12월 미 Naval Postgraduate School 연구조교수. 1995년 3월~1999년 8월 한국항공우주연구원 선임연구원. 1999년 9월~2000년 12월 충남대학교 조교수. 2001년 1월~현재 한국과학기술원 항공우주공학전공 부교수. 관심분야는 인공위성 자세제어, 무인항공기 제어, 비행제어 시스템 설계, 비행체 유도 및 제어.